LAND DEGRADATION & DEVELOPMENT
Land Degrad. Develop. (2017)
Published online in Wiley Online Library (wileyonlinelibrary.com) **DOI**: 10.1002/ldr.2703

MORPHOLOGICAL SIMILARITY OF CHANNELS: FROM LINEAR EROSIONAL FEATURES (RILL, GULLY) TO ALPINE RIVERS

Giulia Sofia[1]*, Costanza Di Stefano[2], Vito Ferro[3], Paolo Tarolli[1]

[1]*Department Land, Environment, Agriculture, and Forestry, University of Padova, Agripolis, Viale dell'Università 16, Padova, Italy*
[2]*Department of Agricultural and Forestry Sciences, University of Palermo, Viale delle Scienze 90128 Palermo, Italy*
[3]*Department of Earth and Marine Sciences, University of Palermo, Via Archirafi 20, 90123 Palermo, Italy*

Received 30 September 2016; Revised 10 January 2017; Accepted 7 February 2017

ABSTRACT

The geometric characteristics of incised features such as channels, rills, ephemeral gully, gully, represent the erosional transport regime and the fluvial dynamic equilibrium, and thus it is critical for the understanding of the long-term evolution of natural, agricultural, and anthropogenic landscapes. This paper examines the morphological similarity of channelized erosion in two different environments such as Alpine landscapes and cultivated hillslopes. The first dataset comprises six rivers in the Italian Alps, three in the Carnia region and three in the Dolomites, where erosion is mainly the effect of discharges with high sediment loads or landslides and debris flows. The agricultural areas dataset includes rills, ephemeral gullies, and gullies surveyed in literature. This research highlights that the eroded volume in Alpine rivers is in line with that of agricultural landscapes or badlands around the world. Dolomites rivers of colluvial origin, flowing on soils that are not particularly deep and subject to natural disaggregation, tend to behave similarly to ephemeral gullies. Contrarily, channels that exhibit evident alluvial morphologies and coarse grain sizes are more similar to gully erosion. At different spatial scales, the results demonstrated that length–volume equations calibrated on rills, ephemeral gullies, gullies and badlands, might be feasible also for Alpine channels. The research areas present soils and bedrock lithology that differs from those in literature, thus suggesting that the morphology of linear erosion is independent of the intrinsic soil characteristics. Differences emerged between Dolomites and Carnia rivers: this highlights the importance of taking into account in future analyses other forcing factors (e.g. climate) on land degradation processes. Copyright © 2017 John Wiley & Sons, Ltd.

KEY WORDS: soil erosion; channel geometry; channelized erosion on hillslopes; rivers; erosion measurement; channelized erosion on hillslopes

INTRODUCTION

Understanding linear erosional features, such as rills (RLs), ephemeral gullies (EGs), gullies (Gs), or river channels, is an important issue for a good catchment management (Mekonnen *et al.,* 2015), and for the analysis of the long-term dynamics of natural, agricultural (Boardman, 2013; Gallart *et al.,* 2013; Bagarello *et al.,* 2015; Caraballo-Arias *et al.,* 2015; Galati *et al.,* 2015; García-Ruiz *et al.,* 2015; Ben Slimane *et al.,* 2016; Selkimäki & González-Olabarria, 2016; Caraballo-Arias & Ferro, 2016; Mwango *et al.,* 2016; Prosdocimi *et al.,* 2016; Prosdocimi *et al.,* 2017), and anthropogenic landscapes (Hancock & Evans, 2010; Tarolli & Sofia, 2016). Indeed, if on the one hand, channel incision controls the evolution of the landscape (Capra *et al.,* 2009), on the other, the channel shape is set by the past and current patterns of erosion (Stark, 2006) and its controlling factors. Researchers have been increasingly investigating the geometric characteristics of channel reaches (Graf, 1983; Montgomery & Gran, 2001; Pitlick & Cress, 2002; Wohl *et al.,* 2004; Rubin *et al.,* 2006; Wohl & Merritt, 2008; Pike *et al.,* 2010; Wilcox *et al.,* 2011; Sutfin *et al.,* 2014). Some authors showed that erosion processes could be parameterized for RLs, EGs, and Gs considering different scale factors (Casali *et al.,* 1999; Nachtergaele *et al.,* 2001; Capra *et al.,* 2005, 2009, 2011; Bruno *et al.,* 2007; Kirkby, 2010; Di Stefano & Ferro, 2011; Capra, 2013; Di Stefano *et al.,* 2013). However, much of this work has been in disturbed or agricultural settings (Hancock & Evans, 2010) where erosion is influenced by the resistance of the topsoil (Knapen & Poesen, 2009) and by agricultural practices (Di Stefano & Ferro, 2016). Conversely, fluvial systems produce discernible patterns across different landscapes (Whiting *et al.,* 1999; Wohl *et al.,* 2004; D'Agostino & Vianello, 2005; Vianello & D'Agostino, 2007; Wohl & Merritt, 2008). Their erosion patterns have been analysed in areas where they differ from linear features in time scale and factors controlling their occurrence and evolution (tectonics, climate, anthropogenic activities) (Attal *et al.,* 2011). Yet, the variability of geometries derived by erosive processes among different environments, such as cultivated hillslopes or high steep alpine terrains, has received less attention, and thus it is still an open research topic. Even though both fluvial systems and linear features (rill, ephemeral gully, and gully) are known to produce a high amount of sediment, little attention has been given to the similarities of the erosional features within these two distinct environments, and thus implicit laws must still be developed for the erosion in both cultivated areas and alpine landscapes.

*Correspondence to: G. Sofia, Department Land, Environment, Agriculture, and Forestry, University of Padova, Agripolis, Viale dell'Università 16, Legnaro (PD), Italy.
E-mail: giulia.sofia@unipd.it

The aim of this paper is to analyse the morphological similarity between RLs, EGs, Gs, and some alpine rivers. The research benefits from the latest advance in geomorphometry (Sofia *et al.,* 2016) and high-resolution topography (Tarolli, 2014) from Laser Scanning, and from the availability of published data from literature (Daba *et al.,* 2003; Capra *et al.,* 2005, 2011; Cheng *et al.,* 2006; Zhang *et al.,* 2007; Bagarello *et al.,* 2008, 2013; Bruno *et al.,* 2008; Moges & Holden, 2008; Di Stefano & Ferro, 2011). More in detail, the length–volume relationships theoretically deduced (Bruno *et al.,* 2008) and calibrated for channelized erosion in cultivated landscapes (Di Stefano & Ferro, 2011; Di Stefano *et al.,* 2013) are applied to test the morphological similarity of channelized erosion features occurring in different environments.

MORPHOMETRIC CHARACTERIZATION OF CHANNELIZED EROSIONAL FEATURES

Gullies (Gs) are defined as isolated features that cut into a smooth pre-existing surface, composed of deep channels on a hillside, rectangular or V-shaped in cross section, generally cut by running water, and often not containing a perennial flow (Kirkby & Bracken, 2009).

Smaller erosional channels with discontinuous flow pathways can be defined as RLs if they are usually eliminated by tillage or natural seasonal processes and do not reoccur at the same location (Carson & Kirkby, 1972). Rills are differentiated from EGs that occur along the axis of a well-defined hollow or thalweg, and can re-form in the same location in successive storms, and are therefore likely to enlarge over time (Bull & Kirkby, 1997).Several researchers (Ichim *et al.,* 1990; Casali *et al.,* 1999; Nachtergaele *et al.,* 2001; Capra *et al.,* 2005, 2009, 2011; Zucca *et al.,* 2006; Zhang *et al.,* 2007; Moges & Holden, 2008; Muñoz-Robles *et al.,* 2010; Di Stefano & Ferro, 2011; Caraballo-Arias *et al.,* 2012, 2014; Mukai, 2016; Di Stefano *et al.,* 2016) found that, in a given study area, an accurate prediction of the length L of channelized erosion features may be sufficient to predict accurately the eroded volume V, given that an empirically derived relationship of L–V is available, as in

$$V = a_s \, L^{b_s} \tag{1}$$

Where: V is the volume (of the gully or other feature) in m^3, L is the length in m, and a_s and b_s are coefficients empirically derived.Linear erosion processes derived by a rainfall of intensity i, acting on a soil having a bulk density ρ_s and characteristic particles diameter d_{50}, and producing a reach r,s (RLs, EGs, Gs) of a given length $L_{r,s}$, volume $V_{r,s}$, width w and maximum depth H, can be expressed by the following function (Bruno *et al.,* 2008; Di Stefano & Ferro, 2011):

$$f\left(V_{r,s},\ L_{r,s},\ w,\ H,\ \rho_s,\ d_{50},\ i\right) = 0 \tag{2}$$

in which f is a functional symbol.Using $L_{r,s}$, ρ_s, i as dimensionally independent variables and applying the Π-Theorem of the dimensional analysis (Barenblatt, 1987, 1996), Equation 2 can be transformed into

$$\phi\left(\frac{V_{r,s}}{L_{r,s}^3},\ \frac{w}{L_{r,s}},\ \frac{H}{L_{r,s}},\ \frac{d_{50,}}{L_{r,s}}\right) = 0 \tag{3}$$

in which φ is a functional symbol.

For a given soil (d_{50} constant), the following exact functional relationship of Equation 3 was determined by Bruno *et al.* (2008) by applying the theory of the incomplete self-similarity (Barenblatt, 1987, 1996):

$$\frac{V_{r,s}}{L_{r,s}^3} = a_r \left(\frac{w\ H}{L_{r,s}^2}\right)^{n_r} \tag{4}$$

Where: a_r and n_r are empirically derived constants (Daba *et al.,* 2003; Capra *et al.,* 2005; Cheng *et al.,* 2006; Zhang *et al.,* 2007; Moges & Holden, 2008; Capra *et al.,* 2009; Di Stefano & Ferro, 2011; Capra, 2013; Di Stefano *et al.,* 2016).

In this study, the length–volume relationships theoretically deduced (Equations 1 and 4) and calibrated for channelized erosion in agricultural settings (Di Stefano & Ferro, 2011; Di Stefano *et al.,* 2013) and Badlands (Caraballo-Arias *et al.,* 2014) are applied to test the morphological similarity of channelized erosion features occurring in different environments.

EXPERIMENTAL AREAS

This study analysed various rivers in the Alpine Regions of Dolomites and Carnia, in northern Italy. For the Dolomites, this research considered the Rio Cordon and a colluvial tributary (Figure 1a and b, respectively) and the Rio Cordevole (Figure 1c) (Sofia *et al.,* 2015) in the Veneto region. In Carnia, the analysed areas were the Miozza river (Figure 1 d), the Pontebbana (Figure 1e), and the Dogna (Figure 1f) streams in the Friuli–Venezia Giulia region. For each study site, accurate LiDAR Digital Terrain Models (DTMs) at 1-m resolution are available.

The analysed portion of the Rio Cordon is the final reach of the river, up to the outlet of the catchment, draining about 5·9 km^2 and covering about 2·6 km in length, with an average slope of 15%. For the same watershed, we investigated a small colluvial tributary (Figure 1b), with an approximate length of 1 km and an average channel slope of 20%.

The considered reach of the Rio Cordevole is the final part of the channel upstream the measuring stream-gauge of "La Vizza" (Belluno), and it covers about 2·9 km in length, with an average channel slope of 12%. The drained watershed is about 7·1 km^2.

For the Carnia rivers, the headwater catchment of the Miozza has an area of 4·5 km^2. The investigated channel is 2·3 km long, with an average channel slope of 31%. The investigated stretch of the Pontebbana is the final part of the stream, upstream the city of Graben (Udine), excluding the parts where the tributary enters the Fella river that presents

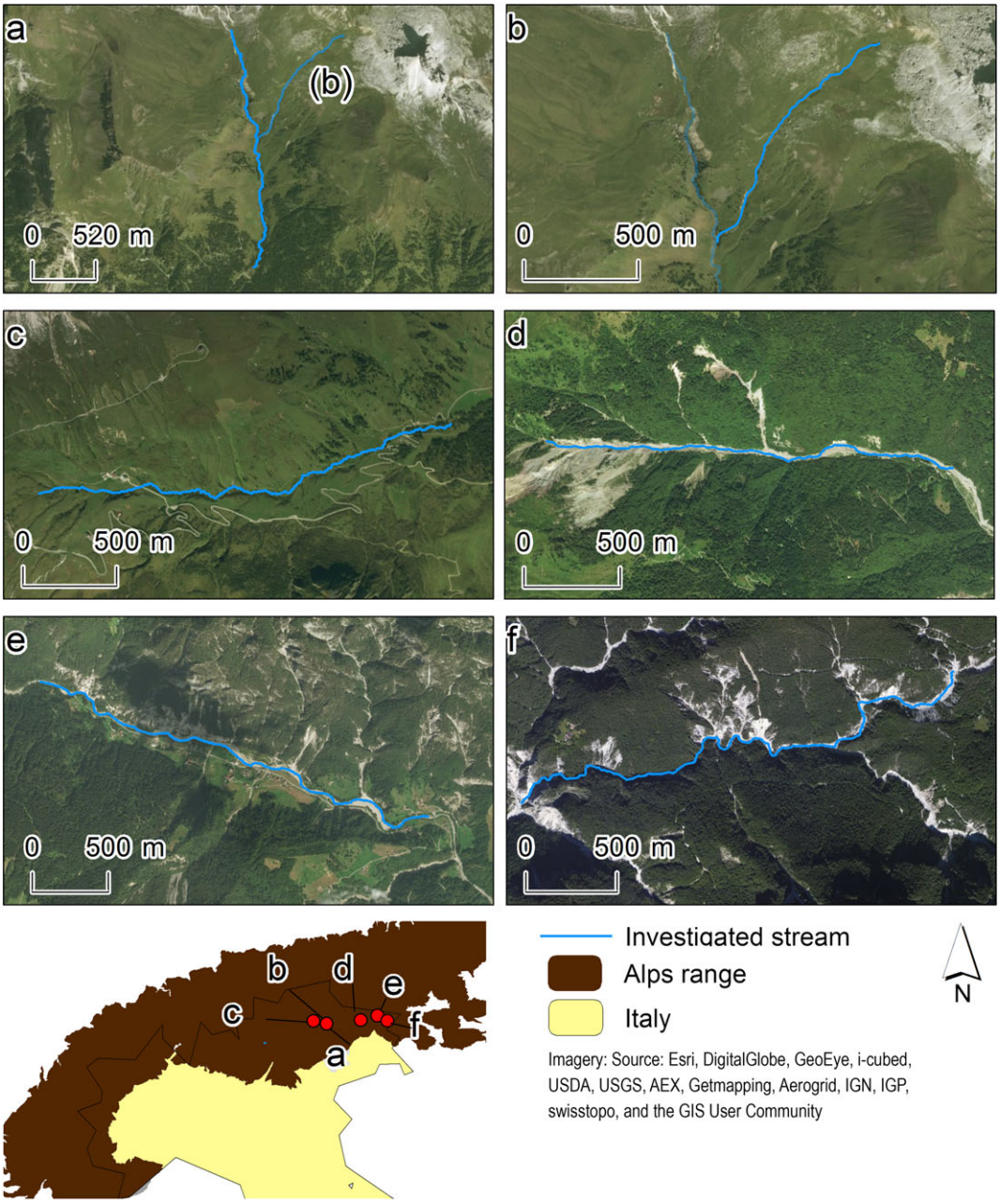

Figure 1. Experimental areas. Dolomites rivers: (a) Rio Cordon, (b) colluvial tributary of Rio cordon, (c) Rio Cordevole. Carnia rivers: (d) Miozza river, (e) Pontebbana, and (f) Dogna torrents. [Colour figure can be viewed at wileyonlinelibrary.com]

engineering structures. The considered channel covers about 3·1 km in length, with an average slope of 3%. The drainage area at the outlet of the channel measures 2·7 km^2. For the Dogna river, the analyses focus on the headwater catchment, covering 4·3 km^2. The stream is about 3·4 km long, with an average channel slope of 10%.

The Rio Cordevole is quite regular, and its width is related to events with recurrence intervals ranging between one and two years (thus fitting the definition of dominant discharge (Wolman & Leopold, 1957; Wolman & Miller, 1960; Vianello & D'Agostino, 2007; Sofia *et al.,* 2015).

For the other study sites, the channel geometry is the result of other shaping factors, and it is highly influenced by a wide range of geomorphic processes such as landslides and debris flows. Both the Rio Cordon (Mao *et al.,* 2005; Comiti *et al.,* 2007; Wilcox *et al.,* 2011) and the Miozza (Tarolli & Tarboton, 2006; Tarolli & Dalla Fontana, 2009) catchments are characterized by floods with heavy solid transport and debris flows, and landslides originating from the combined effects of extreme short rainfalls, low-intensity prolonged rainfalls, and snow melt. Furthermore, the Rio Cordon widths present drastic changes after discharges corresponding to a return period of ~50 years (Lenzi, 2001). The small tributary geometry is also highly shaped by debris flows and landslide events (Tarolli *et al.,* 2012), and by the sediment available at the headwater of

the catchment (visible in Figure 1b). The Dogna catchment is affected by many landslides: Figure 1f shows the landslide-scarred hillslopes after the alluvial events of 22 June 1996, 29 August 2003, and 4 September 2009. The Pontebbana torrent is similarly characterized by landslides driving sediment into the channel. These events hardly shaped the downstream part of the river, due to heavy solid transport. In all these areas, a certain range of discharges defines the bankfull condition, rather than a single value, as found in other steep mountain watersheds (see Radecki-Pawlik, 2002).

METHODS

Width Extraction

Some assumptions must be highlighted, to give a context to the automatic definition of river geometries from a light detection and ranging (LiDAR) DTM. Water largely absorbs the signal from non-bathymetric LiDAR. Thus, on the digital model, the minimum bankfull extent at each location of the stream reflects the width of the channel occupied by water (Sofia *et al.,* 2015). The geometry of each cross section is approximated, depending on the DTM vertical quality, as well as on the depth of water at the time of the survey (Cavalli & Tarolli, 2011). Other works in literature showed that reading the geometries on the DTMs can correctly depict 70% of the total cross sections analysed with a DTM of 3-m resolution, while better performances are expected at higher resolutions, and in steeper areas (Passalacqua *et al.,* 2012). Given these constraints, the proposed method is applied to give an average characterization of the channel geometry, rather than an exact one at each location.

The method for the extraction of widths is based on the procedure described in Sofia *et al.* (2015), and discussing in detail its effectiveness is beyond the scope of this paper. In this research, the core datasets are high-resolution (1 m) LiDAR DTMs, where some of the cross sections extracted with the proposed technique were visually checked to verify the quality of their representation, and to confirm the visibility of the riverbed. As pointed out, the objective of the methodology is an average characterization, rather than an exact one. Thus, it is acceptable that there might be cross sections that are mis-delineated by the automated technique because of the complex nature of channel topography.

The methodology starts from the evaluation of the minimum curvature (Evans, 1972; Evans, 1979; Wood, 1996), which emphasises the concavities of a landscape. The main extraction algorithm can be conceptualized into three steps: (i) definition of homogeneous reaches, and of the hydrologic floodplain; (ii) characterization of transect orthogonal to the thalweg at a reach-scale; and (iii) calculation of the width of each transect and calculation of the reach-scale width. According to Sofia *et al.* (2015), a homogeneous reach comprises a reach where the drainage area constantly increases, as sudden changes in the contributing area are related to lateral intakes from secondary tributaries. The hydrologic plain is defined as the overall size of the valley (total bankfull capacity) where the active channel can flow. The size of the hydrologic plain is chosen automatically, considering the *fitting–enforcing* approach (Sofia *et al.,* 2011; Sofia *et al.,* 2013; Sofia *et al.,* 2015). According to this method, minimum curvature is evaluated using different scales of analysis (kernels, k), and the skewness $skew_k$ of each curvature map is computed. A polynomial function relating the skewness to the kernel size is defined as follows:

$$skew_k = m_o k^n + m_1 k^{(n-1)} + m_2 k^{(n-2)} \ldots + m_n \qquad (5)$$

Where: k is the kernel size, and it is a positive integer odd number ranging from a minimum of 3 to a user-defined maximum ($k_{\max}$), n is a positive integer (degree of the polynomial), $m_o \neq 0$ and m_o ,m_1, m_2, ... m_n are coefficients.The value of n is evaluated at first by fitting the actual skewness values to the kernel size, but it is then iteratively modified (*forced*) until least one value of k exists, within 3 and $k_{\max}$, that maximizes the value of skewness in the negative domain, thus verifying the condition

$$skew'_k = 0 \qquad (6)$$

being $skew'_k$ the first derivative of Equation 5.

The value of $k_{\max}$ should be wide enough to capture the morphology correctly under investigation. Literature suggests that the kernel should be between two and three times the average features size (Pirotti & Tarolli, 2010; Sofia *et al.,* 2011; Tarolli *et al.,* 2012). For the Cordevole river, we considered a $k_{\max}$ of 33 m (Sofia *et al.,* 2015); for the other rivers, we enlarged the range to $k_{\max}$ = 55 m, given that their average widths are around 15–20 m.

Once the floodplain size is evaluated, the above steps are re-computed for each homogeneous reach, assessing the skewness of the minimum curvature values within the floodplain, to define a reach-scale optimum kernel of analysis. For each homogeneous reach, minimum curvature is computed with the reach-scale optimum kernel. A statistic threshold (Lashermes *et al.,* 2007; Passalacqua *et al.,* 2010; Sofia *et al.,* 2011; Tarolli *et al.,* 2012; Sofia *et al.,* 2015) extracts localized widths on cross sections orthogonal to the thalweg, as the width flanked by the points of intersection between the threshold line, and the minimum curvature profile read along the cross section.

The bankfull width is the average value of widths extracted in each homogeneous reach. The widths measured through the procedure are named w_{bkf}.

Reach Depth, Area, and Volume Estimation

The channel depth H and the cross-sectional area A are evaluated through an automatic procedure based on a *flooding algorithm* (Figure 2) along cross sections of 100 m, perpendicular to the thalweg and measured every 10 m. In Figure 2, for discussion purposes, the cross section is an ideal case of a trapezoidal section. However, the *flooding algorithm* reads the values of elevation from the DTM along a 2D profile, where the x corresponds to the progressive distance along

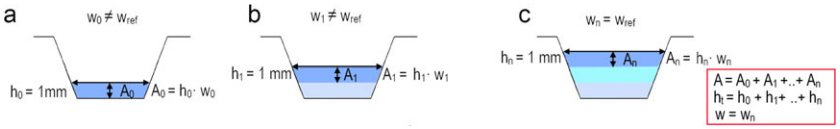

Figure 2. Flooding algorithm schematization. [Colour figure can be viewed at wileyonlinelibrary.com]

the cross section, and y is the elevation in m a.s.l. read at each pixel. Thus, the section shape can vary.

The name of the algorithm derives from the concept of inundation by a flood: the boundaries of the cross section are filled progressively with water (virtually), and eventually the whole section will fill to its maximum capacity, which corresponds to the bankfull width (Figure 2).For each section:

1 it evaluates an initial depth, equal to the elevation of the thalweg, h_n, in m a.s.l.
2 it defines

$$h_i = 0{\cdot}001 \text{ m (Fig. 2a)} \tag{7}$$

3 at each step, it stores h_i and progressively sums it until a specific condition is met

$$h_t = \sum_{i=0}^{n-1} h_i \text{(Fig.2b)} \tag{8}$$

4 it creates a line of equation

$$y = h_t \text{(Fig.2b)} \tag{9}$$

5 it evaluates a temporary bankfull width w_t as the width flanked by the two points of intersection between the line of Equation 9, and the line representing the cross-section elevation profile;
6 assuming to fill the section with water, it evaluates the area of the progressively flooded area as

$$A_t = h_i \;\; w_t \text{(Fig.2b)} \tag{10}$$

7 it stores the values of A_t from Equation 10, and h_t from Equation 8, and repeats steps 2 to 6, until w_t equals a reference width (w_{ref}) (Figure 2c).

For all channels, w_{ref} is set to be equal to the automatically extracted width (w_{bkf}). However, the flooding algorithm can be modified to fit any w_{ref}, thus allowing for comparison of parameters between automatically extracted widths and, as an example, field surveyed ones or widths manually derived from high-resolution aerial photographs.

At the point the condition is met, Equation 8 gives the final cross-section depth.The cross-section area is given by

$$A = \sum_{i=0}^{n} A_{t,i} \tag{11}$$

Moreover; the reach width is

$$w = w_{ref} \tag{12}$$

For each analysed homogeneous reach, identified between two sections r and s, the reach volume $V_{r,s}$ is computed as

$$V_{r,s} = 0.5 \;\; (A_r + A_s) \;\; L_{r,s} \tag{13}$$

Where: A_r and A_s are the area values corresponding to the two cross-sections r and s, calculated by Equation 11, and $L_{r,s}$ is the reach length.

Cumulative volume V and progressive length L are evaluated progressively summing $V_{r,s}$ and $L_{r,s}$ downstream.

Morphological Similarity of Channelized Erosion Features in Different Environments

The similarity of channelized erosion features across landscapes was verified in two steps, to answer to two main questions:

1 What are the coefficients of the length–volume relationships (Equations 1 and 4) that apply to the investigated Alpine rivers?
2 Can the coefficients calibrated and verified in agricultural settings by Di Stefano *et al.* (2013) be applied to the Alpine dataset?

To answer to the first point, the length–volume relationships theoretically deduced (Equations 1 and 4) are fitted and calibrated for the geometries of the Alpine channel reaches. This fitting is accomplished by a non-linear approximation approach based on a Gaussian model. In this method, the parameters of the approximating functions are not necessarily linear on the original function, and they are determined using non-linear optimisation (Dennis, 1996). The fitting automatically calculates optimised start points for Gaussian models based on the fitted data set and imposes no bounds on the resulting coefficients.

Second, the fitting is repeated by imposing as starting point for the optimization the values of the coefficients of Equations 1 and 4 calibrated for Gs and EG (L-V_{Gs} and L-V_{EGs}, respectively) and multiple erosion processes by Di Stefano *et al.* (2013) referencing field surveyed data and other literature data (Ichim *et al.,* 1990; Daba *et al.,* 2003; Moges & Holden, 2008; Di Stefano & Ferro, 2011), and bounding the fitting to the 95% confidence interval of the above-mentioned functions. As a result, imposing these bounds verifies effectively the applicability of a family of curves with specific properties (Taubin *et al.,* 1994), in this case, those of L-V_{Gs} or L-V_{EGs} or all erosive processes, and it establishes if these curves can effectively represent the Alpine dataset.

A two-tailed Student's t-test at $\alpha = 0{\cdot}05$ verifies the validity of the equations.

RESULTS AND DISCUSSION

Length–Volume (L–V) Analysis

Equation 1 was tested and compared to literature values using the cumulative values of L and V of the six considered rivers in a log–log diagram (Figure 3a). Table I reports the estimated a_s and b_s coefficients obtained for each river, as well as for the whole dataset of Carnia and the Dolomites (Figure 3b).

The L–V relationship (Equation 1) presents exponents b_s ranging between ~1 and ~3. The scaling factor (a_s) is highly variable; its minimum value can be found in the Dolomites river Rio Cordevole, while maximum values are for the Rio Cordon channels.

From a physical point of view, the L–V relation of many of the river reaches has values ranging between those of Gs and EGs (Figure 3a). This implies that these rivers might have similar width–depth ratio values. The majority of the Carnia rivers well fit within the confidence bounds of the L–V equation for Gs (Figure 3a and b, Table I). The coefficient b_s calibrated considering all rivers, the Carnia rivers or the Dolomites ones (Figure 3b) well overlap with those of Gs by Di Stefano *et al.* (2013). However, each Dolomitic river presents, for a given length increase, a slightly lower increase in eroded volume than that of a Carnia river (Figure 3a) (smaller b_s).

Fitting the calibrated L-V_{Gs} and L-V_{EGs} (Di Stefano *et al.,* 2013) to the Alpine dataset shows interesting results (Table II). From this analysis, power regression models are obtained which are also characterized by very high determination coefficients and statistically significant R^2 for the L-V_{Gs} equations (Table II). However, by using the L-V_{EGs} bounds, results are never significant.

By bounding the power law, it is interesting to notice that all investigated rivers assume the same value of scaling parameter (a_s = 5·1), which corresponds to the lower limit of the (Di Stefano *et al.,* 2013) L-V_{Gs} equation. Thus, scaling relationships in Alpine rivers might be similar to those of gully erosion, but with a lower eroded volume for a given length.

For the power-law exponent (b_s), results vary among the different rivers. The Carnia rivers appear to be more in line with gully erosion, while the Dolomites rivers are the least similar, but still in line with the literature results. When considering the whole dataset, as found by Caraballo-Arias *et al.* (2014) for Badlands, the L–V measurements in the Alps could also be explained by the application of Equation 1 with constant b_s ~ 1·1 as in Di Stefano & Ferro (2011), Di Stefano *et al.* (2013), & Caraballo-Arias *et al.* (2014), but with a scaling factor that differs of one order of magnitude (a_s = 5·1).

Focusing on the variation in the exponent b_s for Equation 1 for each channel (Table II), the evaluated coefficients are in line with values found in the literature. The lowest exponents are those of the Rio Cordon colluvial tributary and the Rio Cordevole. The Rio Cordon colluvial tributary confidence bounds include the value of b_s found by Zucca *et al.* (2006) for erosion processes on colluvial substrata (1·42) in Sardinia. The exponents of the Rio Cordon, its colluvial tributary and the Rio Cordevole are close to those found for EGs by Cheng *et al.* (2006) & Zhang *et al.* (2007), where, however, the scaling factor a_s was of two orders of magnitude smaller. The exponents of the Carnia rivers (Miozza, Dogna, and Pontebbana) are more close to those of Gs (Casali *et al.,* 1999; Nachtergaele *et al.,* 2001; Capra *et al.,* 2005, 2009, 2011; Zhang *et al.,* 2007; Muñoz-Robles *et al.,* 2010).

Among the investigated Dolomitic rivers, some examples are worth to be analysed more in detail. The Rio Cordevole is characterized, in its upper part ($L \leq$ ~1000 m), by limited

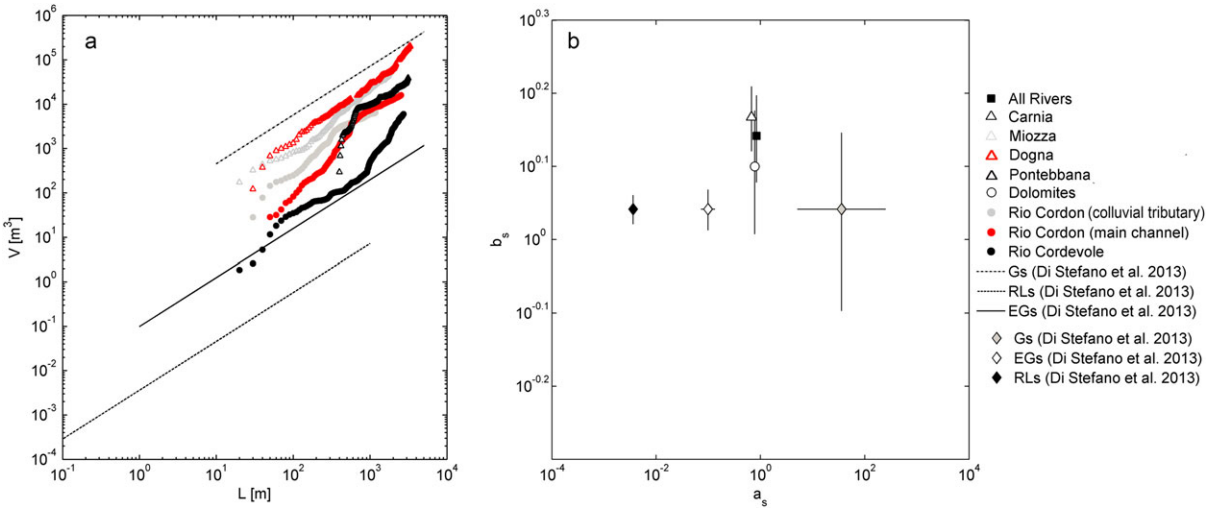

Figure 3. Results of the length–volume (L–V) analysis for gullies (Gs), rills (RLs), and ephemeral gullies (EGs) and the investigated alpine rivers: (a) length–volume relationship derived from literature data (Di Stefano *et al.,* 2013) compared to the alpine dataset; (b) coefficients of equation 1 and their confidence intervals (black lines) calibrated for the investigated sites as compared to literature data (Di Stefano *et al.,* 2013). [Colour figure can be viewed at wileyonlinelibrary.com]

Table I. a_s and b_s coefficients estimated for Equation 1 with R^2 (coefficient of determination), and 95% confidence interval ($CI_{95\%}$) of the fitting, obtained for each channel, and considering the whole dataset (all rivers), the Carnia rivers (Miozza, Dogna, and Pontebbana), and the Dolomites ones (Rio Cordon and its tributary, and Rio Cordevole)

	a_s	$CI_{95\%}$	b_s	$CI_{95\%}$	R^2
Miozza	0·589	0·430–0·747	1·519	1·482–1·555	0·99*
Dogna	0·023	0·016–0·029	1·973	1·937–2·010	0·99*
Pontebbana	2·756	2·145–3·367	1·17	1·141–1·198	0·98*
Rio Cordon (Colluvial Tributary)	11·37	8·232–14·510	0·906	0·865–0·947	0·97*
Rio Cordon (Main channel)	8·116	6·433–9·800	0·971	0·943–0·998	0·98*
Rio Cordevole	4·96E − 06	3·591e − 06–6·319E − 06	2·648	2·613–2·684	1·00*
Carnia rivers	0·675	0·086–1·437	1·47	1·321–1·628	0·54*
Dolomites rivers	0·781	0·505–2·062	1·259	1·017–1·501	0·43*
All rivers	0·847	0·2656–1·960	1·386	1·197–1·575	0·38*

*marks the values of R^2 statistically significant after testing with two-tailed Student's t-tests at $\alpha = 0{\cdot}05$.

Table II. a_s and b_s coefficients estimated for Equation 1 bounded with the Di Stefano *et al.* (2013)$CI_{95\%}$ for the gully L–V relationship. R^2 (coefficient of determination) and 95% confidence interval ($CI_{95\%}$) of the fitting, obtained for each channel, and considering the whole dataset (all rivers), the Carnia rivers (Miozza, Dogna, and Pontebbana), and the Dolomites ones (Rio Cordon and its tributary, and Rio Cordevole)

	a_s	$CI_{95\%}$	b_s	$CI_{95\%}$	R^2
Miozza	5·1	3·309–6·891	1·226	1·178–1·273	0·97*
Dogna	5·1	2·329–7·871	1·288	1·219–1·357	0·93*
Pontebbana	5·1	3·960–6·240	1·09	1·062–1·119	0·98*
Rio Cordon (Colluvial Tributary)	5·1	4·836–5·364	0·906	0·865–0·947	0·80*
Rio Cordon (Main channel)	5·1	4·946–9·800	0·971	0·943–0·998	0·98*
Rio Cordevole	5·1	0·272–10·470	0·836	0·696–0·975	0·68*
Carnia rivers	5·1	0·0027–10·200	1·201	1·068–1·335	0·54*
Dolomites rivers	5·1	0·0114–16·110	0·982	0·593–1·235	0·41*
All rivers	5·1	0·2181–11·810	1·127	0·926–1·309	0·37*

*marks the values of R^2 statistically significant after testing with two-tailed Student's t-tests at $\alpha = 0{\cdot}05$.

vertical incision, and therefore erosion is mostly expended in width adjustment, rather than in channel deepening (Vianello & D'Agostino, 2007; Sofia *et al.,* 2015).

Observing Figure 3a, it appears that the reaches of the Rio Cordevole flowing in these specific morphologic conditions align with the L-V_{EGs} relationships by Di Stefano *et al.* (2013). Bounding the power low equation (Equation 1) and fitting it considering the Rio Cordevole upper part ($L < 1000$ m), the estimated $a_s = 0{\cdot}1063$ ($CI_{95\%} = 0{\cdot}1026$–$0{\cdot}1101$) and $b_s = 1{\cdot}134$ ($CI_{95\%} = 1{\cdot}030$–$1{\cdot}170$) are in line with the L-V_{EGs} relationship (Di Stefano *et al.,* 2013), with high reliability of the power-law equation ($R^2 = 0{\cdot}90$). In the upper part of Rio Cordevole, soils are not particularly deep, but they are subject to natural disaggregation under the action of overland and channelized flows (Vianello & D'Agostino, 2007). This phenomenon, at the upper part of the basin, generates many incisions (RLs) associated with an ephemeral colluvial network from which the Rio Cordevole starts. On the other hand, in the lower portion of the river ($L > 1000$ m), the stream exhibits common boulder bed units, such as cascades and step pool morphologies and presents coarse grain sizes (Vianello & D'Agostino, 2007). This portion fits better with the gully relationship ($a_s = 5{\cdot}100$ [$CI_{95\%} = 3{\cdot}733$–$13{\cdot}970$], $b_s = 0{\cdot}842$ [$CI_{95\%} = 0{\cdot}614$–$1{\cdot}071$], $R^2 = 0{\cdot}61$), while it presents a non-significant relationship ($R^2 \sim 0$) if bounded to the EG equation.

Among the Carnia rivers, the Pontebbana torrent is that more diverging from the gully range of values, especially in its upper part ($L \leq 1000$ m in Figure 3a). The power law fitted to the bottom of the torrent fits in the range of the L-V_{Gs} relationship and provides values of the coefficients $a_s = 5{\cdot}100$ [$CI_{95\%} = 3{\cdot}683$–$6{\cdot}157$], $b_s = 1{\cdot}090$ [$CI_{95\%} = 1{\cdot}055$–$1{\cdot}126$] ($R^2 = 0{\cdot}97$). The upper part of the torrent presents a higher slope of the power-law relationship $b_s = 1{\cdot}692$ [$CI_{95\%} = 1{\cdot}459$–$1{\cdot}9256$] and a scaling value 2–3 orders of magnitude smaller ($a_s = 0{\cdot}095$, $CI_{95\%} = 0{\cdot}053$–$0{\cdot}2434$, $R^2 = 0{\cdot}85$). These values, for this part, seem to be more in line with the values of Badlands (Caraballo-Arias *et al.,* 2012, 2014) ($a_s = 0{\cdot}021$ and $b_s = 2{\cdot}85$). For this river, one must note that the upper part ($L < 1000$ m) is characterized by numerous landslides and debris flow converging into the river bed (Figure 4a). The bottom part instead presents less erosion on the hillslope (Figure 4b).

The upper part is probably characterized by cross sections, which are deeper and wider than the ones of the Gs available in the literature, and of those in the bottom of the river. Thus, the analysis aligns the upper portion of the river

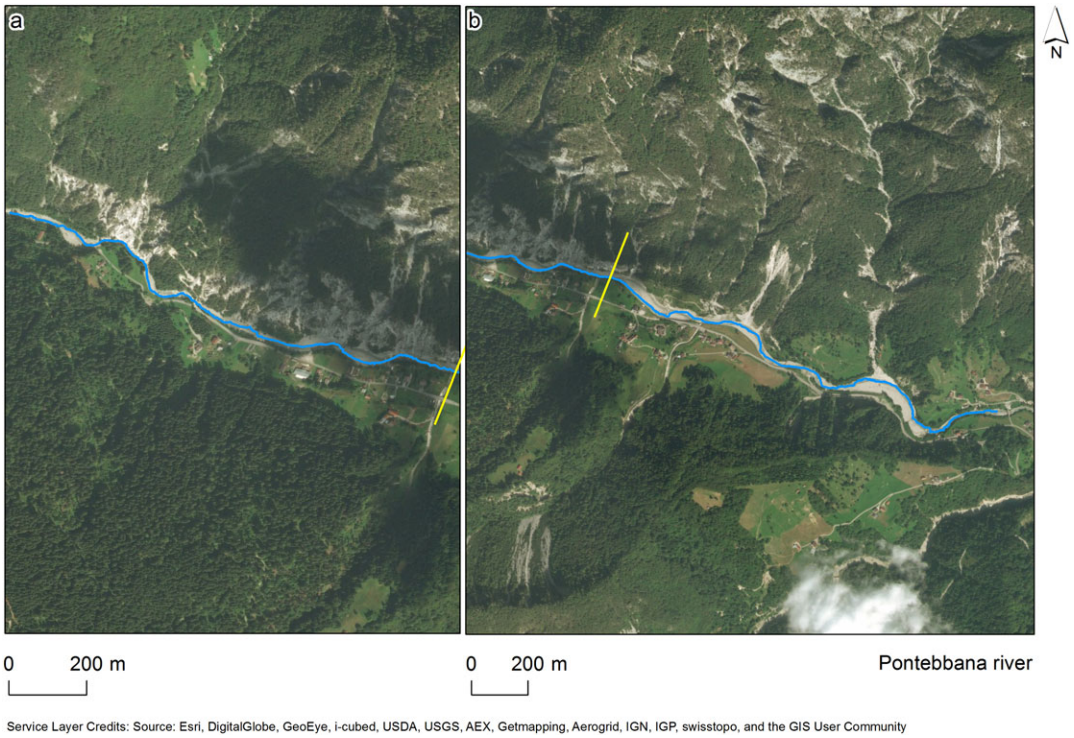

Figure 4. Pontebbana river: upper portion (a), and lower part (b). The yellow line indicates the 1000 m limit for the Pontebbana river.

more to that of Badlands, even if different water erosion processes control the river geometry.

Dimensionless Length–Volume (DL–V) Analysis

Figure 5 shows the analysis of Equation 4 compared to literature values (Di Stefano *et al.,* 2013). Table III shows the values of a_r and n_r fitted for Equation 4.

The analysis of Equation 4 shows that the considered rivers fit mostly into the same range of analysis of that of literature data (Figure 5a). Overall, Carnia, Dolomites rivers and the whole dataset present a scaling factor (a_r) that is in line with that observed for Gs, EGs, and RLs (Di Stefano *et al.,* 2013). As well, comparable values of n_r, are visible (Figure 5b, Table 3). The Dolomites rivers present similar values of n_r, while in general, erosional processes within Carnia channels present a slightly lower value.

The scaling factors a_r of the Carnia rivers (Miozza, Dogna, Pontebbana) and the whole Alpine dataset are in line with those found in different environments by Capra (2013), Caraballo-Arias *et al.* (2014), & Di Stefano & Ferro (2011).

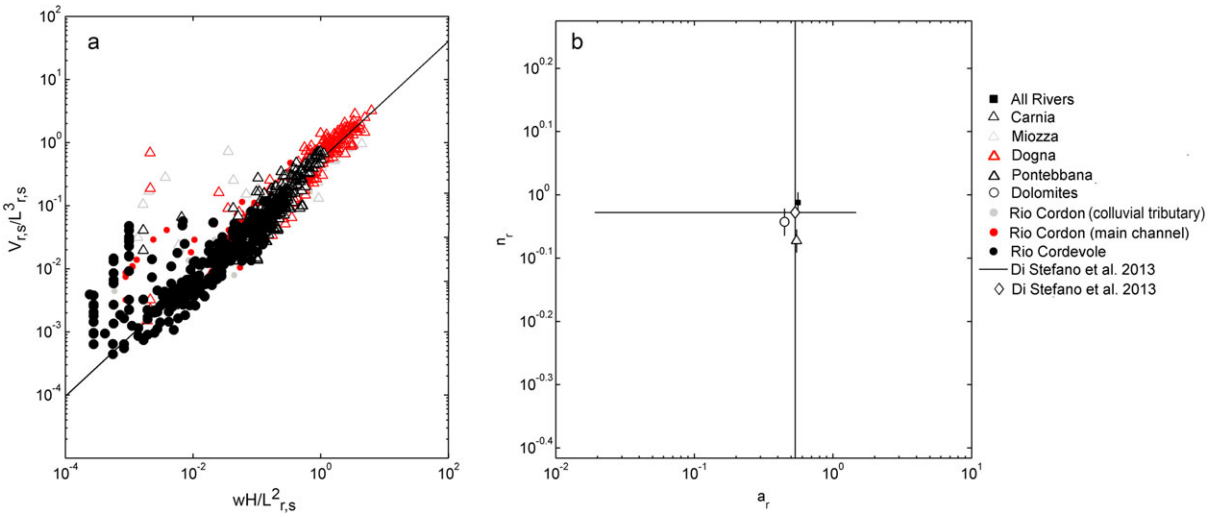

Figure 5. Dimensionless analysis: (a) dimensionless relationship for the literature data (Di Stefano *et al.,* 2013) and the investigated sites; (b) coefficients of Equation 4 and confidence intervals (black lines) as derived for the investigated sites as compared to literature data (Di Stefano *et al.,* 2013). [Colour figure can be viewed at wileyonlinelibrary.com]

Table III. a_r and n_r coefficients estimated for Equation 4 with R^2 (coefficient of determination), and 95% confidence interval ($CI_{95\%}$) of the fitting, obtained for each channel, and considering the whole dataset (all rivers), and the Carnia rivers (Miozza, Dogna and Pontebbana) and the Dolomites ones (Rio Cordon and its tributary, and Rio Cordevole)

	a_s	$CI_{95\%}$	b_s	$CI_{95\%}$	R^2
Miozza	0·513	0·482–0·545	0·744	0·664–0·824	0·56*
Dogna	0·627	0·596–0·659	0·832	0·783–0·882	0·83*
Pontebbana	0·646	0·614–0·678	0·802	0·702–0·902	0·83*
Rio Cordon (colluvial tributary)	0·414	0·351–0·476	0·887	0·805–0·971	0·77*
Rio Cordon (main channel)	0·448	0·410–0·487	0·905	0·852–0·957	0·69*
Rio Cordevole	0·299	0·230–0·368	0·802	0·702–0·902	0·64*
Carnia rivers	0·546	0·540–0·582	0·846	0·811–0·881	0·81*
Dolomites rivers	0·447	0·417–0·478	0·907	0·862–0·951	0·79*
All rivers	0·559	0·544–0·574	0·972	0·935–1·01	0·86*

*marks the values of R^2 statistically significant after testing with two-tailed Student's t-tests at $\alpha = 0{\cdot}05$.

The scaling factors of Dolomites, however, present slightly lower values than those reported in the works mentioned above. The dolomitic rivers (aside from the Colluvial tributary of Rio Cordon) present exponents that are more within the ranges found in Casali *et al.* (1999), Nachtergaele *et al.* (2001), Bruno *et al.* (2007), Zhang *et al.* (2007), Capra (2013), & Caraballo-Arias *et al.* (2014), but scaling factors halved than those in the same works.

Table IV shows the fitting of Equation 4 bounded to the Di Stefano *et al.* (2013) values range.

Table IV confirms that Equation 4 fitted using $a_r = 0{\cdot}5341$ and $n_r = 0{\cdot}9379$, calibrated by Caraballo-Arias *et al.* (2014), Di Stefano *et al.* (2013), & Di Stefano & Ferro (2011) on RLs, EGs, Gs, and badlands, might be feasible also for channels having wider sizes such as the Alpine rivers of this research. By bounding the power law, it is interesting to notice that Dolomites rivers (Rio Cordon alluvial and colluvial tributary, and Rio Cordevole) assume the same value of scaling parameter and exponent ($a_r = 5{\cdot}515$ and $n_r = 0{\cdot}944$), which corresponds to the lower limit of a_r and the upper bound of n_r in Di Stefano *et al.* (2013). This highlights how scaling relationships in Dolomitic rivers might be similar to those of other linear erosive processes, but with a lower eroded volume for a given length, and simultaneously a quicker increase of eroded volume at the increase of length. Carnia rivers, on the other hand, tend to align with the upper limit of both a_r and n_r of Di Stefano *et al.* (2013), confirming that they present higher eroded volumes for a given length and simultaneously a quicker increase of eroded volume at the increase of length.

Morphological Similarity of Channels

The above analyses show that a single *L–V* relationship applies indifferently to EGs and Gs and Alpine streams, with changes in the scaling factors. As well, the *DL–V* relationship calibrated for RLs, EGs, Gs, and badlands might be feasible also for channels having wider sizes such as the Alpine rivers of this research. A morphological similarity between Alpine streams and channelized erosion features of other environments, thus, exists.

Among the factors controlling the morphological similarities or differences, soil type appeared to be of importance. Spatial and temporal transitions among river types occur in response to changes in sediment characteristics (Howard *et al.,* 1994). Streams of colluvial origin with shallow soils subject to easy disaggregation tend to align with EGs. Differently, reaches with more prominent alluvial morphologies and coarse grain sizes diverge from EGs. Reaches presenting high sediment loads well align to Gully erosion. Channels in areas where hillslopes produce diffused erosion that couple with the river systems are morphologically similar to badlands.

Table IV. a_r and n_r coefficients estimated for Equation 4 bounded with the Di Stefano *et al.* (2013) $CI_{95\%}$ with R^2 (coefficient of determination), and 95% confidence interval ($CI_{95\%}$) of the fitting, obtained for each channel, and considering the whole dataset (all rivers), and the Carnia rivers (Miozza, Dogna, and Pontebbana) and the Dolomites ones (Rio Cordon and its tributary, and Rio Cordevole)

	a_s	$CI_{95\%}$	b_s	$CI_{95\%}$	R^2
Miozza	0·513	0·482–0·545	0·932	0·932–0·944	0·53*
Dogna	0·554	0·515–0·554	0·932	0·932–0·944	0·83*
Pontebbana	0·554	0·515–0·554	0·944	0·932–0·944	0·83*
Rio Cordon (colluvial tributary)	0·515	0·441–0·589	0·944	0·863–1·03	0·73*
Rio Cordon (main channel)	0·515	0·410–0·487	0·944	0·852–0·957	0·69*
Rio Cordevole	0·515	0·396–0·633	0·944	0·840–1·05	0·55*
Carnia rivers	0·554	0·533–0·574	0·943	0·884–1·01	0·87*
Dolomites rivers	0·515	0·515–0·554	0·907	0·932–0·944	0·78*
All rivers	0·552	0·539–0·563	0·944	0·932–0·944	0·81*

*marks the values of R^2 statistically significant after testing with two-tailed Student's t-tests at $\alpha = 0{\cdot}05$.

Further dissimilarities are explained by the local scale factors controlling Alpine rivers. Channel widening and deepening are controlled by sediment transports, strong hillslope-channel coupling, the occurrence of vertically oscillating bedforms (Wohl & Merritt, 2008), bedrock outcrops, coarse bed sediments limiting the vertical incision (Vianello & D'Agostino, 2007), and limited sediment supply (Whiting *et al.,* 1999). Thus, erosion might develop alternatively (not necessarily simultaneously) by the enlargement of the river itself or by its deepening, resulting in a lower increase in erosion for a given increase in length if compared to linear erosional features.

Climate might also play a major role. Gully processes are commonly triggered or accelerated by extreme climatic events (Valentin *et al.,* 2005). Conversely, Alpine fluvial systems are controlled by the response to discharges with different recurrence intervals (Wolman & Leopold, 1957), or prolonged recursive events. As a consequence, Gs or EGs might develop over very short time scale compared to the landscape development of the Alpine streams.

Gully processes are also affected by a wide array of factors and processes, including rapid land use changes (Valentin *et al.,* 2005). Conversely, alpine fluvial systems are controlled by response to tectonic deformation, and different stream bed types (bedrock, coarse-bed alluvial, and fine-bed alluvial) differ in factors controlling their occurrence and evolution (Howard *et al.,* 1994)

These differences in time development may have implication to managing degraded landscapes.

CONCLUSIONS

The analysis of Alpine rivers showed that, frequently, eroded volumes within channels are in line with those found in agricultural landscapes or badlands around the world. From a physical point of view, the results show that the majority of the investigated rivers presents cross sections, which are mostly in line with that of Gs available in the literature. In the Dolomites, rivers of colluvial origin with soils that are not particularly deep and subject to easy disaggregation tend to align with EGs. Portions of rivers that exhibit more prominent alluvial morphologies and are characterized by coarse grain sizes diverges by EGs, and for a given length, they present a higher corresponding channel volume, which increases more rapidly at the increase in length. For Carnia rivers, with diffuse erosion and high sediment loads, the erosion processes well align to those of gully erosion. The measurements also confirmed the morphological similarity between the Alpine channels and gully and ephemeral gully erosion by a power dimensionless relationship. The analysed landforms present different soils and bedrock lithology amongst them, and they differ from those reported in the literature, thus suggesting that the morphology of linear erosion is, in general, independent of the intrinsic characteristics of the soil, such as texture, organic content, structure, and permeability. However, differences emerged between Dolomites and Carnia rivers, thus highlight the importance of analysing other forcing factors such as climate and substrate on processes.

REFERENCES

Attal M, Cowie PA, Whittaker AC, Hobley D, Tucker GE, Roberts GP. 2011. Testing fluvial erosion models using the transient response of bedrock rivers to tectonic forcing in the Apennines, Italy. *Journal of Geophysical Research* **116**. https://doi.org/10.1029/2010JF001875.F02005

Bagarello V, Birtone M, Di Piazza G, Ferro V, Giordano G, Pampalone V, Pomilla S. 2008. Verifiche sperimentali della USLE a scala di parcella in Sicilia. *Quaderni di Idronomia Montana* **28/1**: 113–142.

Bagarello V, Ferro V, Pampalone V. 2013. A new expression of the slope length factor to apply USLE-MM at Sparacia experimental area (southern Italy). *Catena* **102**: 21–26. https://doi.org/10.1016/j.catena.2011.06.008.

Bagarello V, Di Stefano C, Ferro V, Pampalone V. 2015. Establishing a soil loss threshold for limiting rilling. *Journal of Hydrologic Engineering* **20**. https://doi.org/10.1061/(ASCE)HE.1943-5584.0001056.C6014001

Barenblatt GI. 1987. Dimensional analysis. Gordon and Breach: New York.

Barenblatt GI. 1996. Scaling, self-similarity, and intermediate asymptotics. Cambridge University Press.

Ben Slimane A, Raclot D, Evrard O, Sanaa M, Lefevre I, Le Bissonnais Y. 2016. Relative contribution of rill/interrill and gully/channel erosion to small reservoir siltation in Mediterranean environments. *Land Degradation & Development* **27**: 785–797. https://doi.org/10.1002/ldr.2387.

Boardman J. 2013. Soil erosion in Britain: updating the record. *Agriculture* **3**: 418–442. https://doi.org/10.3390/agriculture3030418.

Bruno C, Di Stefano C, Ferro V. 2007. Monitoraggio dell'erosione rill a scala di parcella. *Quaderni di Idronomia Montana* **27**: 69–86.

Bruno C, Di Stefano C, Ferro V. 2008. Field investigation on rilling in the experimental Sparacia area, South Italy. *Earth Surface Processes and Landforms* **33**: 263–279. https://doi.org/10.1002/esp.1544.

Bull LJ, Kirkby MJ. 1997. Gully processes and modelling. *Progress in Physical Geography* **21**: 354–374.

Capra A. 2013. Ephemeral gully and gully erosion in cultivated land: a review.

Capra A, Mazzara LM, Scicolone B. 2005. Application of the EGEM model to predict ephemeral gully erosion in Sicily, Italy. *Catena* **59**: 133–146. https://doi.org/10.1016/j.catena.2004.07.001.

Capra A, Di Stefano C, Ferro V, Scicolone B. 2009. Similarity between morphological characteristics of rills and ephemeral gullies in Sicily, Italy. *Hydrological Processes* **23**: 3334–3341. https://doi.org/10.1002/hyp.7437.

Capra A, Di Stefano C, Ferro V, Scicolone B. 2011. Morphological characteristics of ephemeral gullies in Sicily, South Italy. *Landform Analysis* **17**: 27–32.

Caraballo-Arias N, Ferro V. 2016. Assessing, measuring and modeling erosion in 'calanchi' areas. A review. *Journal of Agricultural Engineering* **47**(4): 181–190. https://doi.org/10.4081/jae.2016.573.

Caraballo-Arias N, Conoscenti C, Ferro V. 2012. GIS-morphometric analysis of badlands in Sicily (Italy). *Quaderni di Idronomia Montana* **30**: 311–320.

Caraballo-Arias NA, Conoscenti C, Di Stefano C, Ferro V. 2014. Testing GIS-morphometric analysis of some Sicilian badlands. *Catena* **113**: 370–376. https://doi.org/10.1016/j.catena.2013.08.021.

Caraballo-Arias NA, Conoscenti C, Di Stefano C, Ferro V. 2015. A new empirical model for estimating calanchi erosion in Sicily, Italy. *Geomorphology* **231**: 292–300. https://doi.org/10.1016/j.geomorph.2014.12.017.

Carson MA, Kirkby MJ. 1972. Hillslope form and process. Cambridge University Press: New York. https://doi.org/10.2136/sssaj1973.03615995003700010005x

Casali J, Lopez J, Giráldez J. 1999. Ephemeral gully erosion in southern Navarra (Spain). *Catena* **36**: 65–84. https://doi.org/10.1016/S0341-8162(99)00013-2.

Cavalli M, Tarolli P. 2011. Application of LiDAR technology for rivers analysis. *Italian Journal of Engineering Geology and Environment* : 33–34. https://doi.org/10.4408/IJEGE.2011-01.S-03.

Cheng H, Wu Y, Zou X, Si H, Zhao Y, Liu D, Yue X. 2006. Study of ephemeral gully erosion in a small upland catchment on the inner-Mongolian plateau. *Soil and Tillage Research* **90**: 184–193. https://doi.org/10.1016/j.still.2005.09.006.

Comiti F, Mao L, Wilcox A, Wohl EE, Lenzi MA. 2007. Field-derived relationships for flow velocity and resistance in high-gradient

streams. *Journal of Hydrology* **340**: 48–62. https://doi.org/10.1016/j.jhydrol.2007.03.021.

D'Agostino V, Vianello A. 2005. Identificazione morfodinamica del reticolo idrografico: integrazione fra rilievi di campo e tecniche GIS. *Quaderni di Idronomia Montana, 24. Recenti acquisizioni nel settore delle Sistemazioni Idraulico-Forestali* **24**: 271–290.

Daba S, Rieger W, Strauss P. 2003. Assessment of gully erosion in eastern Ethiopia using photogrammetric techniques. *Catena* **50**: 273–291. https://doi.org/10.1016/S0341-8162(02)00135-2.

Dennis JE. 1996. Numerical methods for unconstrained optimization and nonlinear equations. Society for Industrial and Applied Mathematics SIAM: 3600 Market Street, Floor 6, Philadelphia, PA 19104.John E., Schnabel RB

Di Stefano C, Ferro V. 2011. Measurements of rill and gully erosion in Sicily. *Hydrological Processes* **25**: 2221–2227. https://doi.org/10.1002/hyp.7977.

Di Stefano C, Ferro V. 2016. Establishing soil loss tolerance. an overview. *Journal of Agricultural Engineering*

Di Stefano C, Ferro V, Pampalone V, Sanzone F. 2013. Field investigation of rill and ephemeral gully erosion in the Sparacia experimental area, South Italy. *Catena* **101**: 226–234. https://doi.org/10.1016/j.catena.2012.10.012.

Di Stefano C, Ferro V, Sofia G, Tarolli P. 2016. Morphological similarity of channels having different size: from rills to alluvial channels. Quaderni di Idronomia Montana.

Evans IS. 1972. General geomorphometry, derivatives of altitude, and descriptive statistics. In Spatial analysis in geomorphology, Chorley R~J (ed). Harper & Row; 17–90.

Evans IS. 1979. An integrated system of terrain analysis and slope mapping. *Final Report (Report 6) on Grant DA-ERO-591-73-G0040*. Department of Geography, University of Durham.

Galati A, Gristina L, Crescimanno M, Barone E, Novara A. 2015. Towards more efficient incentives for Agri-environment measures in degraded and eroded vineyards. *Land Degradation & Development* **26**: 557–564. https://doi.org/10.1002/ldr.2389.

Gallart F, Marignani M, Pérez-Gallego N, Santi E, MacCherini S. 2013. Thirty years of studies on badlands, from physical to vegetational approaches. A succinct review. *Catena* **106**: 4–11.

García-Ruiz JM, Beguería S, Nadal-Romero E, González-Hidalgo JC, Lana-Renault N, Sanjuán Y. 2015. A meta-analysis of soil erosion rates across the world. *Geomorphology* **239**: 160–173. https://doi.org/10.1016/j.geomorph.2015.03.008.

Graf WL. 1983. Downstream changes in stream power in the Henry Mountains, Utah. *Annals of the Association of American Geographers* **73**: 373–387. https://doi.org/10.1111/j.1467-8306.1983.tb01423.x.

Hancock GR, Evans KG. 2010. Gully, channel and hillslope erosion—an assessment for a traditionally managed catchment. *Earth Surface Processes and Landforms* **35**: 1468–1479. https://doi.org/10.1002/esp.2043.

Howard AD, Dietrich WE, Seidl MA. 1994. Modeling fluvial erosion on regional to continental scales. *Journal of Geophysical Research—Solid Earth* **99**: 13971–13986. https://doi.org/10.1029/94JB00744.

Ichim I, Mihaiu G, Surdeanu V, Radoane M, Radoane N. 1990. Gully erosion on agricultural lands in Romania. In *Soil erosion on agricultural land. Proceedings of a workshop sponsored by the British Geomorphological Research Group, Coventry, UK, January 1989. 1990 pp. 55–67*

Kirkby MJ. 2010. Distance, time and scale in soil erosion processes. *Earth Surface Processes and Landforms* **35**: 1621–1623. https://doi.org/10.1002/esp.2063.

Kirkby MJ, Bracken LJ. 2009. Gully processes and gully dynamics. *Earth Surface Processes and Landforms* **34**: 1841–1851. https://doi.org/10.1002/esp.1866.

Knapen A, Poesen J. 2009. Soil erosion resistance effects on rill and gully initiation points and dimensions. *Earth Surface Processes and Landforms* **35**: 217–228. https://doi.org/10.1002/esp.1911.

Lashermes B, Foufoula-Georgiou E, Dietrich WE. 2007. Channel network extraction from high resolution topography using wavelets. *Geophysical Research Letters* **34**. https://doi.org/10.1029/2007GL031140.L23S04

Lenzi MA. 2001. Step-pool evolution in the Rio Cordon, Northeastern Italy. *Earth Surface Processes and Landforms* **26**: 991–1008. https://doi.org/10.1002/esp.239.

Mao L, Comiti F, Andreoli A, Lenzi MA, Scussel GR. 2005. Bankfull and bed load effective discharge in a steep boulder-bed channel. In *Sediment Budgets 1, Proceedings of Symposium S1, 7th IAHS Scientific Assembly*189.

Mekonnen M, Keesstra SD, Stroosnijder L, Baartman JEM, Maroulis J. 2015. Soil conservation through sediment trapping: a review. *Land Degradation & Development* **26**: 544–556. https://doi.org/10.1002/ldr.2308.

Moges A, Holden NM. 2008. Estimating the rate and consequences of gully development, a case study of umbulo catchment in southern Ethiopia. *Land Degradation & Development* **19**: 574–586. https://doi.org/10.1002/ldr.871.

Montgomery DR, Gran KB. 2001. Downstream variations in the width of bedrock channels. *Water Resources Research* **37**: 1841–1846. https://doi.org/10.1029/2000WR900393.

Mukai S. 2016. Gully erosion rates and analysis of determining factors: a case study from the semi-arid main ethiopian rift valley. *Land Degradation & Development*. https://doi.org/10.1002/ldr.2532.

Muñoz-Robles C, Reid N, Frazier P, Tighe M, Briggs SV, Wilson B. 2010. Factors related to gully erosion in woody encroachment in South-Eastern Australia. *Catena* **83**: 148–157. https://doi.org/10.1016/j.catena.2010.08.002.

Mwango SB, Msanya BM, Mtakwa PW, Kimaro DN, Deckers J, Poesen J. 2016. Effectiveness Of mulching under *Miraba* in controlling soil erosion, fertility restoration and crop yield in the Usambara Mountains, Tanzania. *Land Degradation & Development* **27**: 1266–1275. https://doi.org/10.1002/ldr.2332.

Nachtergaele J, Poesen J, Steegen A, Takken I, Beuselinck L, Vandekerckhove L, Govers G. 2001. The value of a physically based model versus an empirical approach in the prediction of ephemeral gully erosion for loess-derived soils. *Geomorphology* **40**: 237–252. https://doi.org/10.1016/S0169-555X(01)00046-0.

Passalacqua P, Do Trung T, Foufoula-Georgiou E, Sapiro G, Dietrich WE. 2010. A geometric framework for channel network extraction from lidar: nonlinear diffusion and geodesic paths. *Journal of Geophysical Research—Earth Surface* **115**. https://doi.org/10.1029/2009JF001254.F01002

Passalacqua P, Belmont P, Foufoula-Georgiou E. 2012. Automatic geomorphic feature extraction from lidar in flat and engineered landscapes. *Water Resources Research* **48**. https://doi.org/10.1029/2011WR010958.W03528

Pike AS, Scatena FN, Wohl EE. 2010. Lithological and fluvial controls on the geomorphology of tropical montane stream channels in Puerto Rico. *Earth Surface Processes and Landforms* **35**: 1402–1417. https://doi.org/10.1002/esp.1978.

Pirotti F, Tarolli P. 2010. Suitability of LiDAR point density and derived landform curvature maps for channel network extraction. *Hydrological Processes* **24**: 1187–1197. https://doi.org/10.1002/hyp.7582.

Pitlick J, Cress R. 2002. Downstream changes in the channel geometry of a large gravel bed river. *Water Resources Research* **38**. https://doi.org/10.1029/2001WR000898.34-1-34–11

Prosdocimi M, Cerdà A, Tarolli P. 2016. Soil water erosion on Mediterranean vineyards: a review. *Catena* **141**: 1–21. https://doi.org/10.1016/j.catena.2016.02.010.

Prosdocimi M, Burguet M, Di Prima S, Sofia G, Cerdà A, Terol E, Comino JR, Tarolli P. 2017. Rainfall simulation and structure-from-motion photogrammetry for the analysis of soil water erosion in Mediterranean vineyards. *Science of the Total Environment* **574**: 204–215. https://doi.org/10.1016/j.scitotenv.2016.09.036.

Radecki-Pawlik A. 2002. Bankfull discharge in mountain streams: theory and practice. *Earth Surface Processes and Landforms* **27**: 115–123. https://doi.org/10.1002/esp.259.

Rubin Y, Lunt IA, Bridge JS. 2006. Spatial variability in river sediments and its link with river channel geometry. *Water Resources Research* **42**. https://doi.org/10.1029/2005WR004853.n/a-n/a

Selkimäki M, González-Olabarria JR. 2016. Assessing gully erosion occurrence in forest lands in catalonia (Spain). *Land Degradation & Development*. https://doi.org/10.1002/ldr.2533.

Sofia G, Tarolli P, Cazorzi F, Dalla FG. 2011. An objective approach for feature extraction: distribution analysis and statistical descriptors for scale choice and channel network identification. *Hydrology and Earth System Sciences* **15**: 1387–1402. https://doi.org/10.5194/hess-15-1387-2011.

Sofia G, Pirotti F, Tarolli P. 2013. Variations in multiscale curvature distribution and signatures of LiDAR DTM errors. *Earth Surface Processes and Landforms* **38**: 1116–1134. https://doi.org/10.1002/esp.3363.

Sofia G, Tarolli P, Cazorzi F, Dalla Fontana G. 2015. Downstream hydraulic geometry relationships: gathering reference reach-scale width values from LiDAR https://doi.org/10.1016/j.geomorph.2015.09.002

Sofia G, Hillier JK, Conway SJ. 2016. Frontiers in geomorphometry and earth surface dynamics: possibilities, limitations and perspectives. *Earth Surface Dynamics* **4**: 531–547. https://doi.org/10.5194/esurf-4-531-2016.

Stark CP. 2006. A self-regulating model of bedrock river channel geometry. *Geophysical Research Letters* **33**. https://doi.org/10.1029/2005GL023193.L04402

Sutfin NA, Shaw JR, Wohl EE, Cooper DJ. 2014. A geomorphic classification of ephemeral channels in a mountainous, arid region, southwestern Arizona, USA. *Geomorphology* **221**: 164–175. https://doi.org/10.1016/j.geomorph.2014.06.005.

Tarolli P. 2014. High-resolution topography for understanding earth surface processes: opportunities and challenges. *Geomorphology* **216**: 295–312.

Tarolli P, Dalla Fontana G. 2009. Hillslope-to-valley transition morphology: New opportunities from high resolution DTMs. *Geomorphology* **113**: 1–2, 47-56, https://doi.org/10.1016/j.geomorph.2009.02.006.

Tarolli P, Sofia G. 2016. Human topographic signatures and derived geomorphic processes across landscapes. *Geomorphology* **255**: 140–161. https://doi.org/10.1016/j.geomorph.2015.12.007.

Tarolli P, Tarboton DG. 2006. A new method for determination of most likely landslide initiation points and the evaluation of digital terrain model scale in terrain stability mapping. *Hydrology and Earth System Sciences* **10**: 663–677. https://doi.org/10.5194/hess-10-663-2006.

Tarolli P, Sofia G, Dalla Fontana G. 2012. Geomorphic features extraction from high-resolution topography: landslide crowns and bank erosion. *Natural Hazards*. https://doi.org/10.1007/s11069-010-9695-2.

Taubin G, Cukierman F, Sullivan S, Ponce J, Kriegman DJ. 1994. Parameterized families of polynomials for bounded algebraic curve and surface fitting. *IEEE Transactions on Pattern Analysis and Machine Intelligence* **16**: 287–303.

Valentin C, Poesen J, Yong L. 2005. Gully erosion: impacts, factors and control. *Catena* **63**: 132–153. https://doi.org/10.1016/j.catena.2005.06.001.

Vianello A, D'Agostino V. 2007. Bankfull width and morphological units in an alpine stream of the dolomites (northern Italy). *Geomorphology* **83**: 266–281. https://doi.org/10.1016/j.geomorph.2006.02.023.

Whiting PJ, Stamm JF, Moog DB, Orndorff RL. 1999. Sediment-transporting flows in headwater streams. *Bulletin of the Geological Society of America* **111**: 450–466. https://doi.org/10.1016/j.jappgeo.2015.02.001.

Wilcox AC, Wohl EE, Comiti F, Mao L. 2011. Hydraulics, morphology, and energy dissipation in an alpine step-pool channel. *Water Resources Research* **47**. https://doi.org/10.1029/2010WR010192.W07514

Wohl E, Merritt DM. 2008. Reach-scale channel geometry of mountain streams. *Geomorphology* **93**: 168–185. https://doi.org/10.1016/j.geomorph.2007.02.014.

Wohl E, Kuzma JN, Brown NE. 2004. Reach-scale channel geometry of a mountain river. *Earth Surface Processes and Landforms* **29**: 969–981. https://doi.org/10.1002/esp.1078.

Wolman MG, Leopold LB. 1957. River flood plains: some observations on their formation. Geological Survey Professional Paper: JOUR. U.S.

Wolman MG, Miller JP. 1960. Magnitude and frequency of forces in geomorphic processes. *The Journal of Geology* **68**: 54–74. https://doi.org/10.1086/626637.

Wood J. 1996. The geomorphological characterisation of digital elevation models.phdthesis, University of Leicester.

Zhang Y, Wu Y, Liu B, Zheng Q, Yin J. 2007. Characteristics and factors controlling the development of ephemeral gullies in cultivated catchments of black soil region, Northeast China. *Soil and Tillage Research* **96**: 28–41. https://doi.org/10.1016/j.still.2007.02.010.

Zucca C, Canu A, Della PR. 2006. Effects of land use and landscape on spatial distribution and morphological features of gullies in an agropastoral area in Sardinia (Italy). *Catena* **68**: 87–95. https://doi.org/10.1016/j.catena.2006.03.015.

